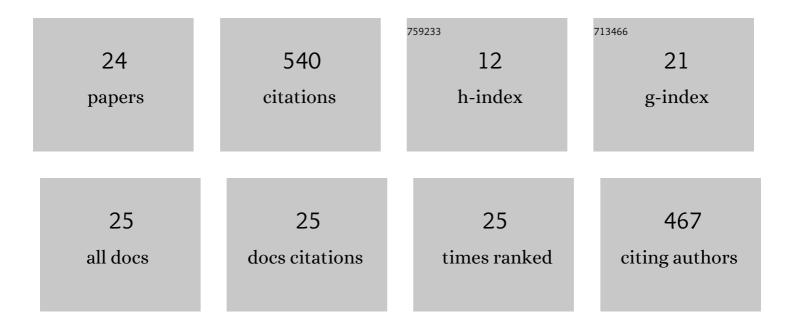
Roman Maniewski

List of Publications by Year in descending order

Source: https://exaly.com/author-pdf/6032759/publications.pdf Version: 2024-02-01



#	Article	IF	CITATIONS
1	Optimal ECG Lead System for Exercise Assessment of Ischemic Heart Disease. Journal of Cardiovascular Translational Research, 2020, 13, 758-768.	2.4	4
2	Assessment of the brain ischemia during orthostatic stress and lower body negative pressure in air force pilots by near-infrared spectroscopy. Biomedical Optics Express, 2020, 11, 1043.	2.9	3
3	High-Resolution Body Surface Potential Mapping in Exercise Assessment of Ischemic Heart Disease. Annals of Biomedical Engineering, 2019, 47, 1300-1313.	2.5	5
4	Influence of intra-abdominal pressure on the amplitude of fluctuations of cerebral hemoglobin concentration in the respiratory band. Biomedical Optics Express, 2019, 10, 3434.	2.9	3
5	Towards in-vivo assessment of fluorescence lifetime: imaging using time-gated intensified CCD camera. Biocybernetics and Biomedical Engineering, 2018, 38, 966-974.	5.9	6
6	Confirmation of brain death using optical methods based on tracking of an optical contrast agent: assessment of diagnostic feasibility. Scientific Reports, 2018, 8, 7332.	3.3	18
7	Application of optical methods in the monitoring of traumatic brain injury: A review. Journal of Cerebral Blood Flow and Metabolism, 2016, 36, 1825-1843.	4.3	64
8	Exercise induced depolarization changes in BSPMs for assessment of ischemic heart disease. , 2015, , .		1
9	Evaluation of T-wave alternans in high-resolution ECG maps recorded during the stress test in patients after myocardial infarction. Archives of Medical Science, 2015, 1, 99-105.	0.9	4
10	ST-segment changes in high-resolution body surface potential maps measured during exercise to assess myocardial ischemia: aÂpilot study. Archives of Medical Science, 2014, 6, 1086-1090.	0.9	4
11	Performance assessment of time-domain optical brain imagers, part 2: nEUROPt protocol. Journal of Biomedical Optics, 2014, 19, 086012.	2.6	85
12	The effect of precordial lead displacement on ECG morphology. Medical and Biological Engineering and Computing, 2014, 52, 109-119.	2.8	69
13	Prolonged Postocclusive Hyperemia Response in Patients with Normal-Tension Glaucoma. Medical Science Monitor, 2014, 20, 2607-2616.	1.1	6
14	Fluorescence-based method for assessment of blood-brain barrier disruption. , 2013, 2013, 3040-2.		8
15	Multiwavelength time-resolved detection of fluorescence during the inflow of indocyanine green into the adult's brain. Journal of Biomedical Optics, 2012, 17, 087001.	2.6	19
16	Time-resolved detection of fluorescent light during inflow of ICG to the brain—a methodological study. Physics in Medicine and Biology, 2012, 57, 6725-6742.	3.0	26
17	Application of a time-resolved optical brain imager for monitoring cerebral oxygenation during carotid surgery. Journal of Biomedical Optics, 2012, 17, 016002.	2.6	35
18	Assessment of inflow and washout of indocyanine green in the adult human brain by monitoring of diffuse reflectance at large source-detector separation. Journal of Biomedical Optics, 2011, 16, 046011.	2.6	41

Roman Maniewski

#	Article	IF	CITATIONS
19	Risk assessment of ventricular arrhythmia using new parameters based on high resolution body surface potential mapping. Medical Science Monitor, 2011, 17, MT26-MT33.	1.1	18
20	Optical system based on time-gated, intensified charge-coupled device camera for brain imaging studies. Journal of Biomedical Optics, 2010, 15, 066025.	2.6	22
21	Body Surface ECG Signal Shape Dispersion. IEEE Transactions on Biomedical Engineering, 2009, , .	4.2	Ο
22	Time-resolved optical imager for assessment of cerebral oxygenation. Journal of Biomedical Optics, 2007, 12, 034019.	2.6	79
23	Evaluation of the QRS-T angle using the high-resolution 64-lead electrocardiography. Anatolian Journal of Cardiology, 2007, 7 Suppl 1, 120-2.	0.4	2
24	Magnetic Measurement of Cardiac Volume Changes. IEEE Transactions on Biomedical Engineering, 1982, BME-29, 16-25.	4.2	16